Anal. Bioanal. Electrochem., Vol. 15, No. 11, 2023, 938-955
https://www.doi.org/10.22034/abec.2023.709095

Analytical & Bioanalytical Electrochemistry

Full Paper

Assessment of The Green Corrosion Inhibition Performances of *Thymus Algeriensis* Microwave-Assisted Extracts on Mild Steel in Acid Solution

Nassima Boutaoui,[1,2] Meryem Acila,[3,*] Hani Boulahbel,[4] Billel Achouri,[4] Lahcene Zaiter,[1] Fadila Benayache,[1] Samir Benayache,[1] Ilaria D'Agostino,[5] Cristina Campestre,[5] and Marcello Locatelli[5]

[1]*Unité de Recherche Valorisation des Ressources Naturelles, Molécules Bioactives et Analyses Physicochimiques et Biologiques, Université Frères Mentouri, Constantine 1, Route d'Aïn El Bey, 25000 Constantine, Algeria*
[2]*Laboratoire de Phytochimie et de Pharmacologie, Département de Chimie, Faculté des Sciences Exactes et Informatique, Université de Jijel, Ouled Aïssa, BP 98, 18000 Jijel, Algeria*
[3]*Laboratoire des Interactions Matériaux Environnement (LIME), Département de Chimie, Faculté des Sciences Exactes et Informatique, Université de Jijel, Ouled Aïssa, BP 98, 18000 Jijel, Algeria*
[4]*Scientific and Technical Research Center in Physico-Chemical Analysis, BP 384, Headquarters ex-Pasna Zone Industrielle Bou-Ismail CP 42004 Tipaza, Algeria*
[5]*Department of Pharmacy, University "G. d'Annunzio" of Chieti-Pescara, Via dei Vestini 31, 66100 Chieti, Italy*

*Corresponding Author, Tel.: +213778154401
E-Mail: acila.meryem@univ-jijel.dz

Received: 24 July 2023 / Received in revised form: 20 October 2023 / Accepted: 18 November 2023 / Published online: 30 November 2023

Abstract- The diversity of extractable compounds provides a potentially rich source of high-value products. The corrosion inhibition performances of seven *Thymus algeriensis* extracts on mild steel in 0.5 M HCl were investigated using the gravimetric method, electrochemical measurements, and surface analysis. The results indicate that the addition of all the extracts significantly decreases the corrosion rate of mild steel with efficiency proportional to the extract concentration. A maximum percentage of inhibition was obtained for the microwave-assisted aqueous extract (T = 100 °C, extraction time = 15 minutes) at a concentration of 500 ppm, which is the most phenolics-enriched extract. Potentiodynamic polarization curves show that the extracts acted as mixed-type corrosion inhibitors and slowed down the anodic and cathodic reaction kinetics. Scanning electron microscopy confirms the presence of a protective

film. The inhibition properties were attributed to the synergism of the active components of the extracts, mainly flavonoids, carotenoids, chlorophylls, and phenolic compounds with functional groups such as conjugated double bonds, aromatic rings, and heteroatoms, which adsorb on the metal surface of the mild steel to form a protective layer preventing the contact of the aggressive medium.

Keywords- Corrosion; green inhibitors; *Thymus algeriensis*; Impedance spectroscopy; Microwave-assisted extraction; SEM

1. INTRODUCTION

Everything around us is susceptible to deterioration [1]. When the destructive attack is carried out by physicochemical or even biological means, it involves swelling or aging of the plastic, rotting of the wood, or even erosion of the granite [2]. On the other hand, when the irreversible deterioration of metal takes place through chemical or electrochemical reactions, corrosion occurs leading to the alteration of the material properties [3].

Nowadays, steel has taken a prominent place in our lives. Indeed, thanks to its low manufacturing cost, and its good mechanical and thermal properties, this material is found in different shapes and sizes, for many and varied applications: the oil and gas industry, the automotive industry, and many other industrial fields [4,5]. However, mild steel suffers from corrosion and the characteristic is significant in industries as production stoppage, replacement of corroded parts, accidents, and risks of pollution are frequent events with sometimes heavy economic consequences [6].

The use of specific inhibitors is one of the most practical methods for corrosion protection, especially in acidic solutions. However, those from synthetic sources are very expensive and mostly dangerous. The non-toxic and biodegradable features of natural-product derivatives have led to their use as green inhibitors [7-10].

Natural products such as compounds extracted from plants seem to be an ideal ecological alternative to replace traditional corrosion inhibitors [11-13]. The present work aims to investigate for the first time the effect of microwave-assisted extracts of *Thymus algeriensis* obtained in different conditions (temperature ranging from 40 to 120 °C, extraction time from 5 to 15 minutes, solvent: water or ethanol/water 50/50) as green corrosion inhibitors on the behavior of mild steel in acidic solution. Different techniques have been used to confirm the anticorrosion efficiency of these extracts such as weight loss methods and electrochemical methods including potentiodynamic polarization and impedance spectroscopy. Scanning electron microscopy (SEM) was used to examine the metal surface's morphology following exposure to an aggressive environment both without and with the addition of inhibitors.

2. EXPERIMENTAL SECTION

Microwave-assisted extracts **T40**, **T60**, **T80**, **T100**, **T120** (extraction time 10 minutes, water as solvent), **T100/5 min** (extraction time 5 minutes, water as the solvent), and **T100/15**

min (extraction times 15 minutes, ethanol/water 50/50 as the solvent) were reported previously by us [14].

2.1. Electrode preparation

Commercial mild steel was used with the following chemical composition (percentage by weight, wt%): 0.04% Mn, 0.39% C, 0.09% P, 0.32% Si, 0.02% Al, 0.04% S and Fe balance. The sample with 1 cm^2 of exposed area was mounted in epoxy resin. Before measurement, the samples were mechanically polished using a series of silicon carbide emery papers (between 600 and 2000 grades), cleaned with distilled water, degreased with acetone, and then dried before immersion in the corrosive solution (0.5 M HCl).

2.2. Electrolyte composition

The corrosion behavior of mild steel was studied in an acidic solution (0.5 M HCl) with and without inhibitor addition. The used concentrations of the extracts were 100, 200, 300, and 500 ppm.

2.3. Gravimetric study

To measure the weight loss, the steel samples were immersed in beakers containing 0.5 M HCl solution. This was done both in the absence of extracts and in the presence of four different concentrations of each extract (100, 200, 300, and 500 ppm). The samples were then sanded sequentially with 600, 800, and 1200 grit fine sandpaper, rinsed with deionized water, and degreased with acetone. Finally, the weight of the washed coupon was measured using a digital balance with an accuracy of 0.1 mg and this weight was recorded as m1. Following that, the samples were submerged in aerated test solutions at 25 °C for three days before being taken out, rinsed with acetone for one minute, washed with distilled water, dried, and then reweighed (m2). The corrosion rate was calculated from equation 1 [15]:

$$\mathrm{CR} = \frac{\Delta m}{\mathrm{S\,x\,t}} \qquad (1)$$

where Δm is the difference between m_1 and m_2 measured in grams, S is the total surface of the specimen in cm^2 and t represents the immersion time in days. The surface coverage, represented as θ, and the percentage inhibition efficiency, denoted as IE, were determined using the equations (2) and (3), respectively [16-18]:

$$\theta = \frac{CR_0 - CR}{CR_0} \quad (2)$$

CR_0 stands for the corrosion rate of the samples without inhibitor addition, while CR represents the corrosion rate of the samples in the presence of the inhibitor.

$$IE = \frac{CR_0 - CR}{CR_0} x100 \quad (3)$$

2.4. Electrochemical tests

Electrochemical experiments were conducted using a Radiometer Analytical Voltalab 40 PGZ301 potentiostat/galvanostat, which was controlled by Voltamaster 4 software. These experiments were carried out in a standard three-electrode cell, with mild steel serving as the working electrode, platinum mesh as the counter electrode, and a saturated calomel electrode (SCE) used as the reference electrode. The polarization curves were recorded after 60 min of immersion in the test solution. Electrochemical Impedance Spectroscopy (EIS) spectra were recorded between 100 kHz and 10 mHz frequency range, using an applied AC signal of 10 mV at the OCP. The data were analyzed and fitted using ZSimpWin software.

2.5. Surface analysis

The surface morphologies of treated and untreated samples were observed using the SEM model ZEISS EVO 15 after immersion in an aggressive environment for 7 days. Before immersing the samples, they underwent a series of polishing steps, starting with silicon carbide paper of various grade numbers ranging from 600 to 1200. Subsequently, a further polishing step was carried out using diamond paste to achieve a nearly mirror-like surface finish. After being immersed for a period of 7 days, the test coupons were retrieved, rinsed with distilled water, dried, and promptly subjected. to analysis.

3. RESULTS AND DISCUSSION

Although most of the studies on plants and in general natural sources are addressed to discovering and, then, developing bioactive compounds for a medicinal purpose, their biodiversity and wide polypharmacology offer several inputs for different applications. This is extremely true for the presence of natural constituents, such as polyphenols, flavonoids, alkaloids, glycosides, etc, that are largely studied as antioxidant agents.

In the Lamiaceae family, *Thymus* emerges for the versatile use that men make of it as both a medicinal and aromatic plant. In fact, it finds several applications as a condiment and culinary spice, but also as an essential oil for its antioxidant, anti-inflammatory, antimicrobial, anticancer, and age-delaying properties [19]. *T. algeriensis* represents one of the most known North African *Thymus* species. Due to the great interest in the biological and pharmacological properties of *Thymus* and, in particular, *T. algeriensis*, the phytochemical composition has been largely investigated, and several protocols for extraction of the main components have been developed [20,21].

In the last years, pollution and chemicals waste are dramatically increasing and great efforts are trying to address the issue by resorting to more eco-friendly activities and developing greener alternatives to traditional life-routinary products, such as cleaning detergents, car fuels, etc, also due to the more and more restrictive environmental regulations. In this field, recently,

producers and users are trying to replace the till-now used chemical anticorrosive agents with greener ones, even if their numerous vantages also include high efficiency. In fact, their high operating cost and hazardous environmental effects promoted the study of non-toxic and environmentally sustainable anticorrosive agents, especially nature-based [22].

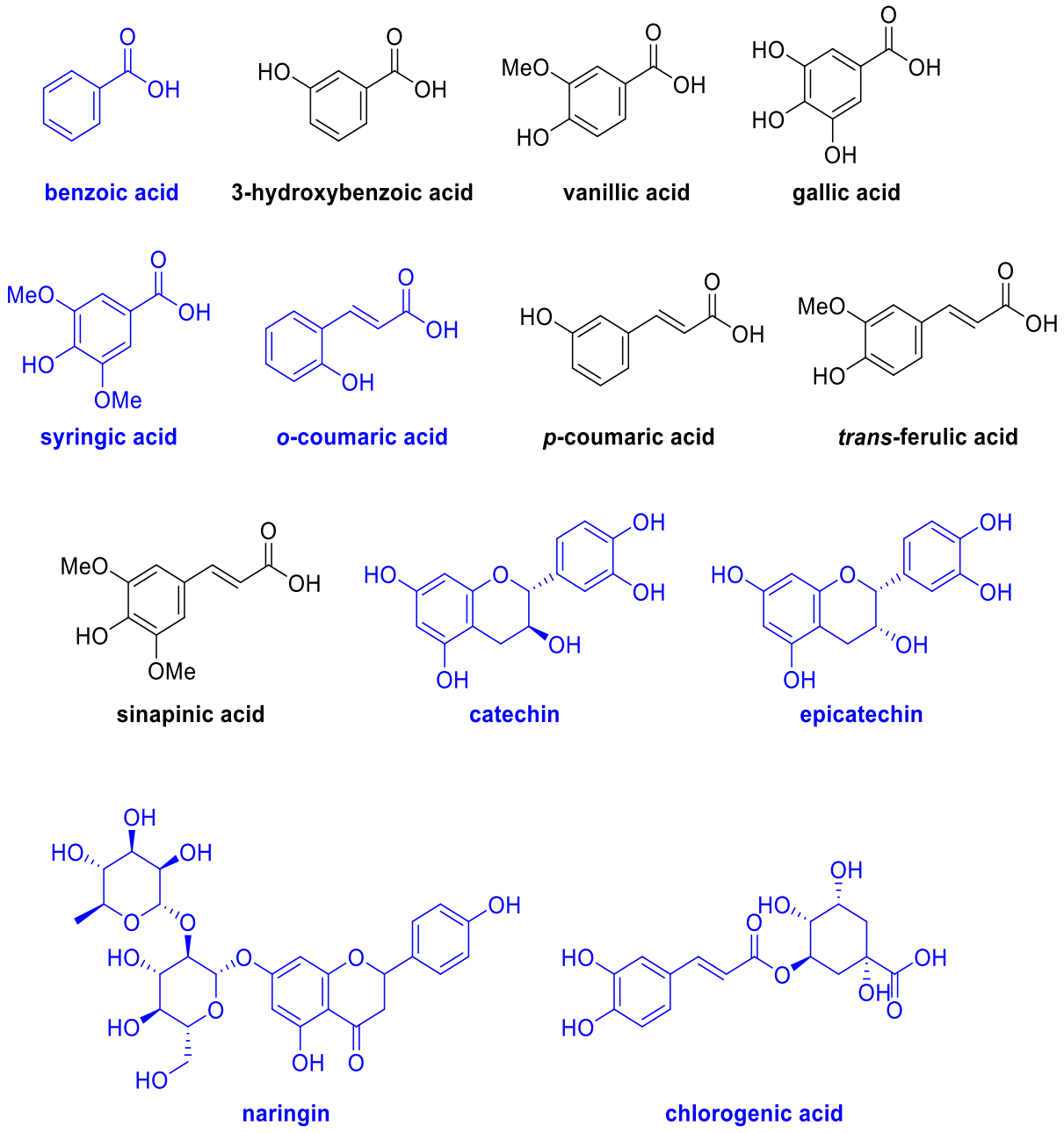

Figure 1. Main components of microwave-assisted extracts from *T. algeriensis*. In blue the most abundant compounds.

In this frame, besides the conventional uses of *T. algeriensis*, this diverse and new scientific application is in development and some research groups have already reported the use of its extracts as corrosion inhibitors for aluminum alloy [18] and mild steel [23].

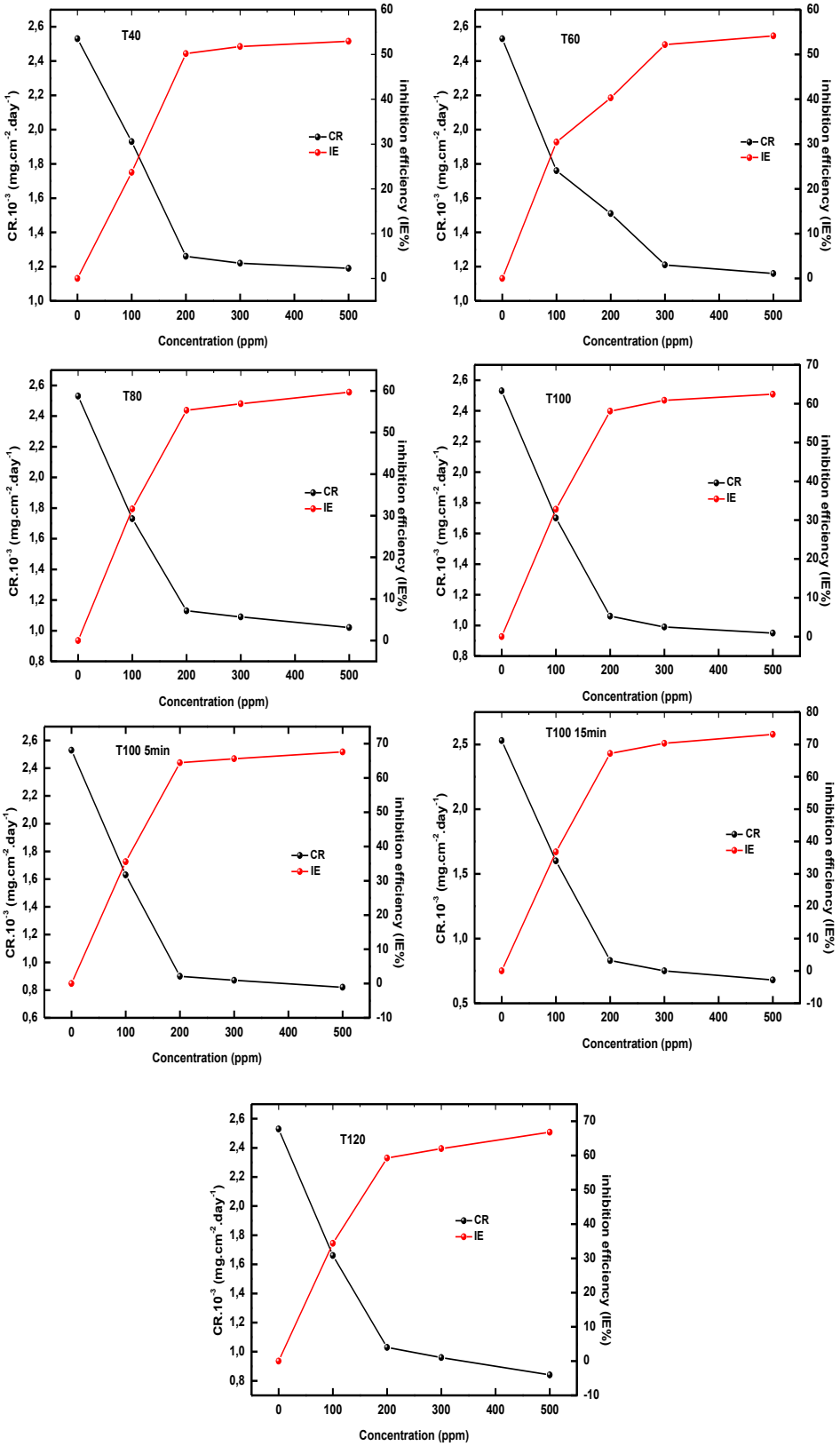

Figure 2. Evolution of the corrosion rate (CR) and inhibition efficiency (IE) of mild steel in 0.5 M HCl solution for different concentrations of extracts

Attracted by its high potentiality not only in the MedChem field, we have been involved in the study and characterization of microwave-assisted extracts of *T. algeriensis*. In particular, we obtained seven extracts, namely T40, T60, T80, T100, T120, T100/5 min, and T100/15 min and characterized their complex mixture of phenolic acids, carotenoids, chlorophylls, and flavonoids, identifying benzoic acid (highest concentration), epicatechin, chlorogenic acid, syringic acid, naringin, catechin, *o*-coumaric acid, and also gallic acid, vanillic acid, *p*-coumaric acid, sinapinic acid, *trans*-ferulic acid, 3-hydroxybenzoic acid, and (Figure 1) as the main components [14].

Herein, we assessed the ability of such extracts to inhibit the corrosion of commercial mild steel by different assays.

Table 1. Corrosion rate and inhibition efficiency for mild steel in 0.5 M HCl solution with different concentrations of extracts obtained from gravimetric measurements

Sample/extract	C (ppm)	CR	θ	IE (%)
Blank	0	$2.53 \cdot 10^{-3}$	0	0
T40	100	$1.93 \cdot 10^{-3}$	0.23	23.71
	200	$1.69 \cdot 10^{-3}$	0.33	33.20
	300	$1.22 \cdot 10^{-3}$	0.42	51.79
	500	$1.19 \cdot 10^{-3}$	0.52	52.96
T60	100	$1.76 \cdot 10^{-3}$	0.30	30.43
	200	$1.51 \cdot 10^{-3}$	0.40	40.32
	300	$1.21 \cdot 10^{-3}$	0.52	52.18
	500	$1.16 \cdot 10^{-3}$	0.54	54.15
T80	100	$1.73 \cdot 10^{-3}$	0.31	31.62
	200	$1.13 \cdot 10^{-3}$	0.55	55.33
	300	$1.09 \cdot 10^{-3}$	0.56	56.92
	500	$1.02 \cdot 10^{-3}$	0.59	59.68
T100	100	$1.70 \cdot 10^{-3}$	0.32	32.81
	200	$1.06 \cdot 10^{-3}$	0.58	58.10
	300	$0.99 \cdot 10^{-3}$	0.60	60.87
	500	$0.95 \cdot 10^{-3}$	0.62	62.45
T100/5 min	100	$1.63 \cdot 10^{-3}$	0.35	35.57
	200	$0.90 \cdot 10^{-3}$	0.64	64.43
	300	$0.87 \cdot 10^{-3}$	0.65	65.61
	500	$0.82 \cdot 10^{-3}$	0.67	67.59
T100/15 min	100	$1.60 \cdot 10^{-3}$	0.36	36.76
	200	$0.83 \cdot 10^{-3}$	0.67	67.19
	300	$0.75 \cdot 10^{-3}$	0.70	70.35
	500	$0.68 \cdot 10^{-3}$	0.73	73.12
T120	100	$1.66 \cdot 10^{-3}$	0.34	34.39
	200	$1.03 \cdot 10^{-3}$	0.59	59.29
	300	$0.96 \cdot 10^{-3}$	0.62	62.05
	500	$0.84 \cdot 10^{-3}$	0.66	66.80

C: concentration; CR: corrosion rate; **θ**: surface coverage; IE: inhibition efficiency; T40, T60, T80, T100 and T120: Thymus extracts at 40, 60, 80,100 and 120°C; T100/5min and T100/15min: Thymus extracts at 100°C for 5 and 15 min.

3.1. Weight loss test

The influence of the addition of each extract at different concentrations on the corrosion rate of mild steel and the corresponding inhibition efficacy is shown on Figure 2.

All the extracts inhibit the corrosion of steel in the acidic medium. The weight loss and the corrosion rate decrease, whereas the inhibitory efficiency increases with the increase in the concentration of inhibitors (Table 1) to reach maximum values of 73.12% and 67.59% for T100/15 min and T100/5 min, respectively, at 500 ppm.

The decrease in the corrosion rate and the increase in the inhibitor efficiencies with the inhibitor concentration is due to the adsorption of inhibitor molecules on the metal surface as indicated by the increase of the surface coverage (θ), which increases with the inhibitor concentration. This behavior may be due to the active sites in the mild steel being blocked by active molecules that reduce the attack of corrosive solutions on the metal surface.

3.2. Potentiodynamic polarization curves

Figure 3 depicts potentiodynamic polarization curves of mild steel without and with the various concentrations of extracts. It is observed that the shape of the curves is almost identical for all the extracts and the addition of the various extracts systematically results in a reduction in the cathodic and anodic current densities. The inhibition efficiency IE (%) obtained from potentiodynamic polarization curves was calculated according to the following equation:

$$\%IE = \frac{i^0_{corr} - i_{corr}}{i^0_{corr}} \times 100 \quad (4)$$

where $i°_{corr}$ is the corrosion current density in the absence of the inhibitor while i_{corr} is that with inhibitor addition. Electrochemical parameters such as e_{corr}, i_{corr}, R_p together with inhibitor efficiency, are shown in Table 2.

It is clear that the values of current densities (i_{corr}) decreased with increasing the concentration of the inhibitors. It passes from 112 mA cm^{-2} for the blank to 18.17 mA cm^{-2} for T100/15 min, 19.32 mA cm^{-2} for T120 and 34.72 mA cm^{-2} for T100/5 min in the presence of inhibitors at 500 ppm. Moreover, the inhibitory efficiency improved with the increase in the concentration of inhibitors. The T100/15 min extract is the most effective. The inhibitory efficacy changes in the following order: T100/15 min > T120 > T100 > T100/5 min > T80 > T60 > T40 which can be explained by the richness of T100/15 min extract in phenolic acids and flavonoids (11 phenolic compounds and 5 flavonoids were previously identified in this extract) [14].

The anodic and cathodic polarization curves show that the addition of these inhibitors leads to a decrease in the anodic and cathodic current densities and slightly modifies the corrosion potential values (E_{corr}). These experimental results confirm that these extracts are mixed inhibitors since the displacement of the corrosion potential E_{corr} in the presence of different

concentrations of the extracts is less than 85 mV compared to the corrosion potential of the blank [24-30].

Table 2. Electrochemical parameters obtained from polarization curves after immersion the electrodes in 0.5 M HCl solution without and with extracts at different concentrations

Sample/extract	C (ppm)	E_{corr} (mV)	i_{corr} (μA cm^{-2})	*Rp* (Ω cm^2)	EI (%)
Blank	-	-389	112	153	-
T40	100	-385	77.52	210	30.78
	200	-360	72.35	227	35.40
	300	-359	69.41	263	38.03
	500	-252	66.37	267	40.74
T60	100	-380	67.43	259	39.79
	200	-379	55.21	316	50.70
	300	-376	47.89	333	57.24
	500	-371	42.19	369	62.33
T80	100	-381	71.62	228	36.05
	200	-362	52.81	320	52.85
	300	-377	48.03	365	57.12
	500	-374	39.58	394	64.66
T100	100	-435	61.32	285	45.25
	200	-456	49.35	336	55.94
	300	-458	44.73	379	60.06
	500	-459	32.06	502	71.37
T100/5 min	100	-379	63.29	279	43.49
	200	-372	47.90	364	57.23
	300	-383	43.56	382	61.10
	500	-381	34.72	488	69.00
T100/15 min	100	-377	41.34	432	63.09
	200	-369	31.16	513	72.18
	300	-373	24.63	687	78.00
	500	-372	18.17	774	83.77
T120	100	-364	65.21	269	41.77
	200	-355	33.62	497	69.98
	300	-353	29.36	536	73.78
	500	-353	19.32	751	80.96

C: concentration; E_{corr}: corrosion potential; i_{corr}: current densities; *Rp*: polarization resistance; EI: inhibition efficiency.

This result clearly indicates that the addition of the inhibitors reduces the anodic dissolution of iron (oxidation to Fe^{2+}) and slows down the evolution of the discharge of protons (H^+), which can be explained by the adsorption of organic compounds present in the extracts forming a protective layer adsorbed on the metal surface.

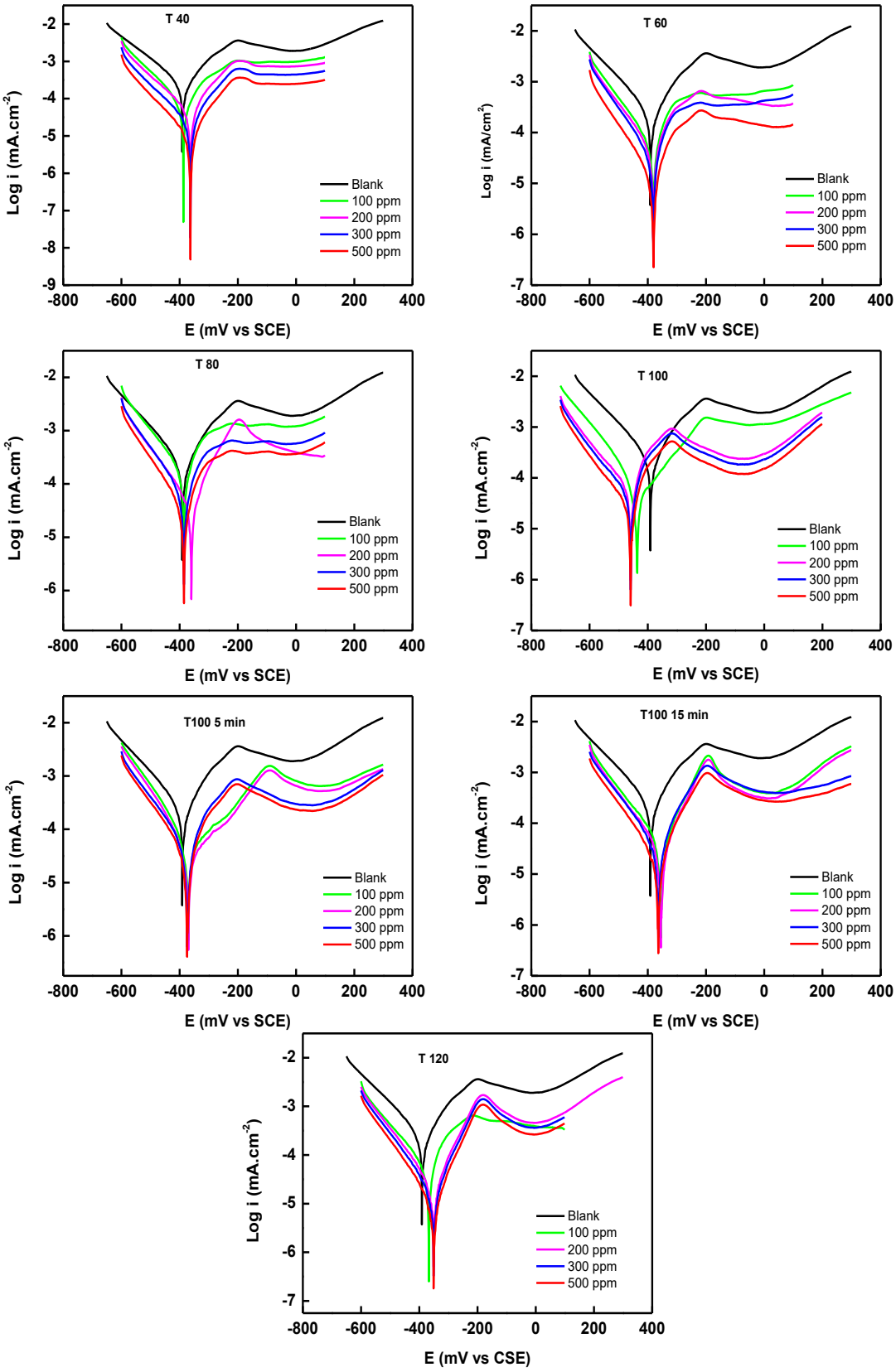

Figure 3. Polarization curves of mild steel in 0.5 M HCl in the absence and in the presence of *T. algeriensis* extracts at different concentrations.

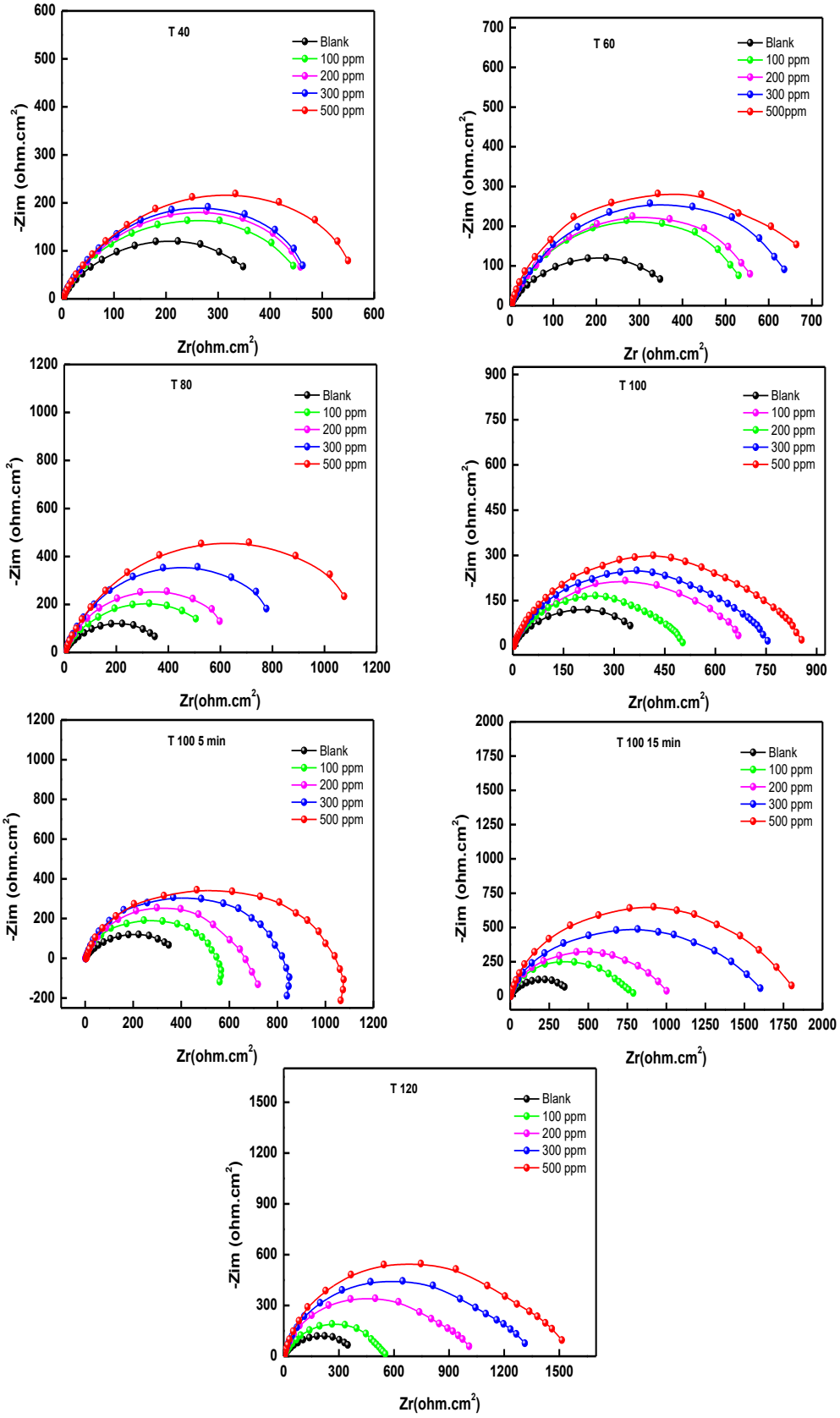

Figure 4. EIS spectra for mild steel corrosion in 0.5 M HCl without and with different concentrations of *T. algeriensis* extarcts

3.3. Electrochemical impedance spectroscopy (EIS)

Nyquist plots of mild steel in the presence and the absence of various concentrations of all the extracts are given in Figure 4.

From the figures, we can see that the impedance diagrams display single capacitive semicircles, showing that the corrosion process is specially controlled by charge transfer [31] . For more details of the impedance spectra, we used the equivalent electrochemical circuit, shown in Figure 5.

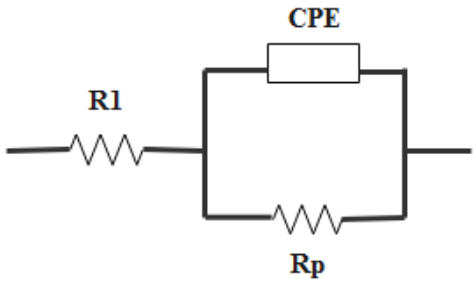

Figure 5. Equivalent electric circuit

This circuit has been used by many authors to explain the behavior of mild steel in acidic solutions [8,11,32,33]. In this circuit, R_1 represents the electrolyte resistance, *Rp* is the charge transfer resistance, and CPE is the double electrochemical layer.

Due to the inhomogeneous nature of the electrode surface, ideal capacitance such as C_{dl} is replaced by constant phase elements, CPE, whose impedance is calculated by:

$$ZCPE = (Q(J\omega)^n)^{-1} \quad (5)$$

where Q is the CPE ($S.sn.cm^{2-}$); ω is the angular frequency (rad/s); n is the CPE index ranging from 1 (pure capacitor) to 0.5 (ideal resistor) [32,34]. After considering the non-uniformity of the electrode surface, the real capacitance was obtained by the following expression:

$$C = Q(\omega_{max})^{n-1} \quad (6)$$

where ω_{max} is the maximum frequency, at which the imaginary component of the Nyquist plot is maximum. However, in the presence of the extracts, the diameter of the semicircles increased with the increase of the extract concentration and Cdl levels fell, suggesting a reduction of the dielectric constant of the metal solution interface by the deposition of inhibitive molecules forming an adherent protective film on the metal surface [35]. The *Rp* values were used to calculate the inhibition efficiency percentage (IE%) using equation (7):

$$\frac{Rp-Rp^{\circ}}{Rp} \times 100 \quad (7)$$

R_p and $R_p°$, respectively, represent the polarization resistance in the presence and absence of extract. According to the results obtained (Table 3), T100/15 min is the most promising extract. Indeed, inhibition efficiency greater than 82% was obtained at a concentration equal to 500 ppm.

Table 3. EIS parameters for mild steel in 0.5 M HCl solution with different concentrations of extracts

Sample/extract	C (ppm)	R_1 ($\Omega.cm^2$)	Rp ($\Omega.cm^2$)	CPE	α	χ^2	IE (%)
Blank		11.36	341	$8.43 \cdot 10^{-4}$	0.94	$6.80 \cdot 10^{-4}$	
T40	100	10.84	465	$9.24 \cdot 10^{-5}$	0.93	$4.60 \cdot 10^{-4}$	26.66
	200	10.92	493	$7.50 \cdot 10^{-5}$	0.91	$4.71 \cdot 10^{-4}$	30.83
	300	11.36	525	$7.40 \cdot 10^{-5}$	0.92	$1.83 \cdot 10^{-4}$	35.05
	500	11.38	569	$2.69 \cdot 10^{-5}$	0.94	$3.98 \cdot 10^{-4}$	40.07
T60	100	12.47	570	$5.62 \cdot 10^{-5}$	0.89	$3.84 \cdot 10^{-4}$	40.17
	200	10.98	710	$4.06 \cdot 10^{-5}$	0.88	$6.20 \cdot 10^{-4}$	51.97
	300	13.25	750	$2.54 \cdot 10^{-5}$	0.87	$1.04 \cdot 10^{-3}$	54.33
	500	11.37	860	$2.21 \cdot 10^{-5}$	0.92	$2.31 \cdot 10^{-3}$	60.35
T80	100	10.74	510	$5.72 \cdot 10^{-6}$	0.89	$3.19 \cdot 10^{-4}$	33.14
	200	13.45	748	$4.98 \cdot 10^{-6}$	0.94	$1.41 \cdot 10^{-3}$	54.41
	300	12.31	775	$4.52 \cdot 10^{-5}$	0.91	$2.37 \cdot 10^{-3}$	56.00
	500	11.56	898	$3.17 \cdot 10^{-5}$	0.87	$4.13 .10^{-4}$	62.03
T100	100	11.23	612	$6.03 \cdot 10^{-5}$	0.91	$5.32 \cdot 10^{-4}$	44.28
	200	12.41	735	$5.39 \cdot 10^{-6}$	0.88	$7.21 \cdot 10^{-4}$	53.60
	300	13.21	849	$2.70 \cdot 10^{-5}$	0.94	$3.25 \cdot 10^{-3}$	59.83
	500	11.57	1198	$2.12 \cdot 10^{-5}$	0.89	$9.71 \cdot 10^{-4}$	71.53
T100/5 min	100	10.65	593	$9.23 \cdot 10^{-6}$	0.90	$8.14 \cdot 10^{-4}$	42.49
	200	11.87	785	$7.26 \cdot 10^{-5}$	0.89	$1.65 \cdot 10^{-3}$	56.56
	300	17.35	843	$5.32 \cdot 10^{-5}$	0.89	$8.37 \cdot 10^{-4}$	59.55
	500	16.65	1120	$4.14 \cdot 10^{-5}$	0.87	$9.31 \cdot 10^{-4}$	69.55
T100/15 min	100	11.56	910	$7.85 \cdot 10^{-6}$	0.87	$7.25 \cdot 10^{-4}$	62.53
	200	12.85	1113	$5.69 \cdot 10^{-5}$	0.89	$6.83 \cdot 10^{-4}$	69.36
	300	13.08	1710	$3.24 \cdot 10^{-5}$	0.88	$5.62 \cdot 10^{-4}$	80.06
	500	17.52	1965	$1.36 \cdot 10^{-5}$	0.92	$2.69 \cdot 10^{-3}$	82.65
T120	100	11.58	590	$8.74 \cdot 10^{-5}$	0.94	$4.38 \cdot 10^{-4}$	42.20
	200	12.69	1117	$3.69 \cdot 10^{-5}$	0.90	$2.79 \cdot 10^{-3}$	69.47
	300	18.02	1420	$2.98 \cdot 10^{-5}$	0.98	$3.87 \cdot 10^{-3}$	75.98
	500	17.26	1597	$1.98 \cdot 10^{-5}$	0.97	$7.21 \cdot 10^{-4}$	78.65

C: concentration; R_1: electrolyte resistance; Rp: polarization resistance; CPE: constant phase elements; α: describes the distribution of the dielectric relaxation time in the frequency domain; χ^2: chi-squared; EI: inhibition efficiency.

The inhibition efficiency of these extracts follows the following order: T100/15 min > T120 > T100 > T100/5 min> T80> T60> T40, in full agreement with the potentiodynamic polarization study.

3.4. Adsorption isotherms

The surface coverage values (θ) for different concentrations of extracts, obtained from gravimetric measurements in 0.5 M HCl medium at 25 °C, were used to study the adsorption process of the different extracts. The plot of $C_{inh/\theta}$ as a function of C_{inh} is linear (Fig. 6) and the correlation coefficient (R^2) is always close to 1 ($R^2 > 0.9912$).

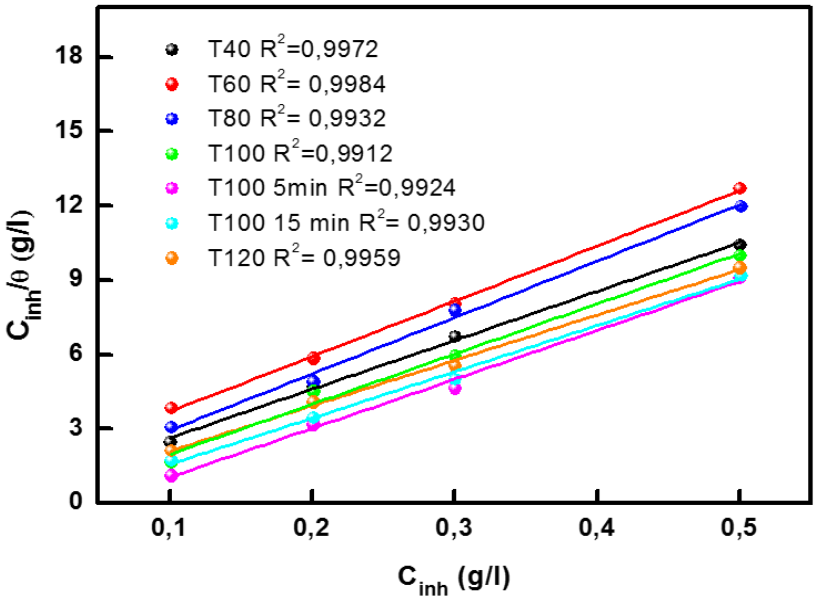

Figure 6. Langmuir plot for mild steel in 0.5 M HCl with different concentrations of *T. algeriensis* extracts at 25 °C

From the plots, we can say that the adsorption of the active molecules of the extracts obeys the Langmuir model, given by the following equation:

$$\frac{C_{inh}}{\theta} = \frac{1}{K_{ads}} + C_{inh} \qquad (8)$$

where C_{inh} is the inhibitor concentration and K_{ads} is the adsorption equilibrium constant. The adsorption equilibrium constant K_{ads} is related to the standard free energy of adsorption $\Delta G°_{ads}$ by the relation below:

$$K_{ads} = \frac{1}{55,5}\, e^{\frac{-\Delta G_{ads}}{R.T}} \qquad (9)$$

The value 55.5 is the concentration of water in solution in mol L^{-1}, and R is the universal gas constant in J/molK and T is the temperature in kelvin (K). The corrosion inhibition b organic compounds can be explained by the criterion 20/40; the values of $\Delta G°_{ads}$ around -20 $KJmol^{-1}$ are consistent with the electrostatic interaction between charged organic molecules and the charged metal surface (physisorption). The values around -40 $KJmol^{-1}$ involve charge sharing or transfer from the organic molecules to the metal surface to form a coordinate bond (chemisorptions) and those between [-20, -40 $kJmol^{-1}$] are attributed to mixed adsorption. However, recent studies confirm that the standard free energy of adsorption may not be a reliable criterion to distinguish between physisorption and chemisorption and this parameter is not sufficient to comprehended mechanism of the adsorption of plant extracts, because the molecular mass is unknown [16,27,36,37,38].

3.5. Surface analysis

In order to observe the morphology of the metal surface in an acidic solution in the absence and the presence of 500 ppm of each extract, SEM was applied. The images obtained reflect the harmful effect of the aggressive environment and the protective power of the extracts. As can be seen, Figures 7b clearly shows the damaging action of the aggressive HCl solution.

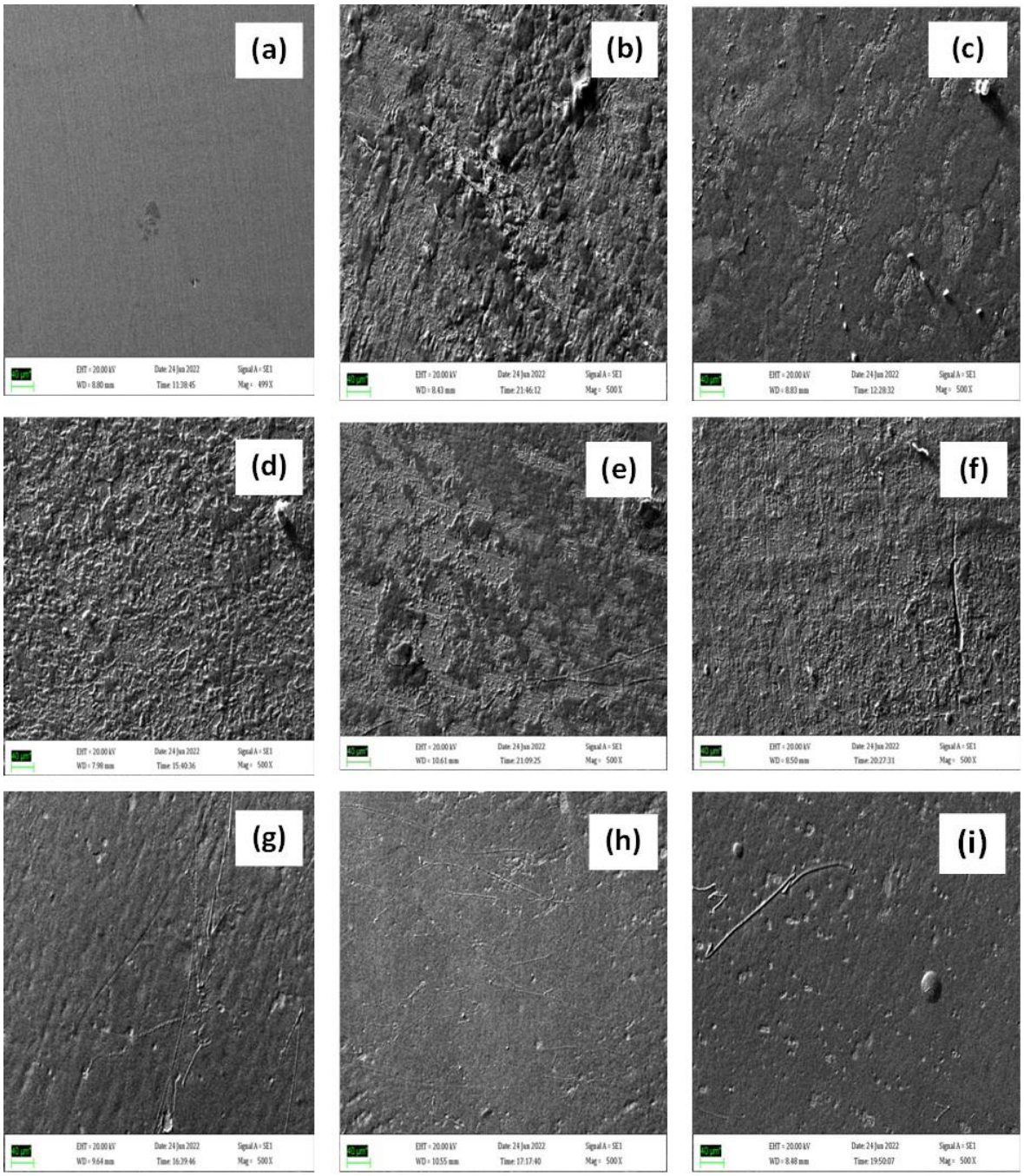

Figure 7. SEM images taken for mild steel before immersion (a), after 7 days immersion in 0.5 M HCl in the absence of inhibitors (b) and in the presence of 500 ppm of *T. algeriensis* extracts: (c) T40, (d) T60, (e) T80, (f) T100, (g) T100/5 min, (h) T100 /15 min, and (i) T120

In the absence of inhibitors, the surface has undergone corrosion and is completely covered by oxidation products. Whereas in the presence of the extracts, as shown in Figure 7, the samples are much less damaged and the surfaces are practically intact in particular with T100/5 min, T100/15 min, and T120. These micrographs clearly show the presence of a deposited film on the metal surface. The latter is due to the adsorption of inhibitor molecules on the steel surface leading to corrosion inhibition.

4. CONCLUSION

The main objective of this study was to propose new green corrosion inhibitors for mild steel in an acidic environment in order to replace the use of hexavalent chromium-based compounds. The principal conclusions achieved are:

i) MAE extracts from *T. algeriensis* show good inhibitive action for mild steel corrosion in 0.5 M HCl; *ii)* the value of the inhibition efficiency (%IE) increases with increasing the inhibitor concentration; *iii)* there is a good agreement between the data obtained from gravimetric and electrochemical methods; *iv)* the adsorption of all MAE extracts on the steel surface obeys to Langmuir adsorption isotherm; *v)* SEM images confirm the ability of *T. algeriensis* extracts to retard the corrosion of mild steel by the formation of an adherent film on metal surface.

Acknowledgments

The authors would like to thank Laboratory of Pharmacy Department, University “G. d’Annunzio” of Chieti-Pescara, for the preparation and caracterisation of MAE extracts.

Declarations of interest

The authors declare no conflict of interest in this reported work.

REFERENCES

[1] Z. Tang, Curr. Opin. Solid State Mater. Sci. 23 (2019) 100759.
[2] H. Keleş, M. Keleş, I. Dehri and O. Serindağ, Colloids Surf. A. Physicochem. Eng. Asp. 320 (2008) 138.
[3] M. Rbaa, and B. Lakhrissi, Surf. Interfaces. 15 (2019) 43.
[4] L. Feng, S. Zhang, L. Hao, H. Du, R. Pan, G. Huang, and H. Liu, Molecules. 27 (2022) 3826.
[5] V. Saraswat, M. Yadav, and I. Obot, Colloids Surf. A. Physicochem. Eng. Asp. 599 (2020) 124881.
[6] Haque, V. Srivastava, C. Verma, and M. Quraishi, J. Mol. Liq. 225 (2017) 848.

[7] C.M. Fernandes, L. Guedes, L.X. Alvarez, A.M. Barrios, H. Lgaz, H.S. Lee, and E.A. Ponzio, J. Mol. Liq. 363 (2022) 119790.
[8] A. Sedik, D. Lerari, A. Salci, S. Athmani, K. Bachari, İ. Gecibesler and R. Solmaz, J. Taiwan Inst. Chem. Eng. 107 (2020) 189.
[9] M. Ferdosi Heragh, and H. Tavakoli, Met. Mater. Int. 26 (2020) 1654.
[10] S. Pal, H. Lgaz, P. Tiwari, I.-M. Chung, G. Ji, and R. Prakash , J. Mol. Liq. 276 (2019) 347.
[11] I. M. Chung, R. Malathy, S. H. Kim, K. Kalaiselvi, M. Prabakaran, and M. Gopiraman, J. Adhes. Sci. Technol. 34 (2020) 1483.
[12] J. Halambek, A.N. Grassino, and I. Cindrić, Int. J. Electrochem. Sci. 15 (2020) 857.
[13] N. Raghavendra, J. Bio. Tribo. Corros. 5 (2019) 54.
[14] N. Boutaoui, L. Zaiter, F. Benayache, S. Benayache, S. Carradori, S. Cesa, A.M. Giusti, C. Campestre, L. Menghini, and D. Innosa, Molecules. 23 (2018) 463.
[15] K. Khaled, Mater. Chem. Phys. 112 (2008) 104.
[16] J. Halambek, K. Berković, and J. Vorkapić-Furač, Mater. Chem. Phys. 137 (2013) 788.
[17] K. Khaled, Mater. Chem. Phys. 125 (2011) 427.
[18] A. Khadraoui, A. Khelifa, K. Hachama, and R. Mehdaoui, J. Mol. Liq. 214 (2016) 293.
[19] I. Mahdi, W.B. Bakrim, G.T.M. Bitchagno, H. Annaz, M.F. Mahmoud, and M. Sobeh, Oxid Med Cell Longev. 2022 (2022).
[20] M. Sobeh, S. Rezq, M. Cheurfa, M.A. Abdelfattah, R.M. Rashied, A.M. El-Shazly, A. Yasri, M. Wink, and M.F. Mahmoud, Biomolecules 10 (2020) 599.
[21] H. Ouakouak, A. Benarfa, M. Messaoudi, S. Begaa, B. Sawicka, N. Benchikha, and J. Simal-Gandara, Plants 10 (2021) 786.
[22] A. Zakeri, E. Bahmani, and A.S.R. Aghdam, Corrosion Communications. 5 (2022) 25.
[23] A. Salhi, A. Bouyanzer, I. El Mounsi, H. Bendaha, I. Hamdani, E. El Ouariachi, A. Chetouani, N. Chahboun, B. Hammouti, and J. Desjobert, J Mater Environ Sci. 7 (2016) 3949.
[24] M. Behpour, S. Ghoreishi, N. Mohammadi, and M. Salavati-Niasari, Corros. Sci. 53 (2011) 3380.
[25] L. Zhou, Y.-L. Lv, Y.-X. Hu, J.-H. Zhao, X. Xia, and X. Li, J. Mol. Liq. 249 (2018) 179.
[26] M. Bouanis, M. Tourabi, A. Nyassi, A. Zarrouk, C. Jama, and F. Bentiss, Appl. Surf. Sci. 389 (2016) 952.
[27] S. Varvara, R. Bostan, O. Bobis, L. Găină, F. Popa, V. Mena, and R.M. Souto, Appl. Surf. Sci. 426 (2017) 1100.
[28] K. Krishnaveni, and J. Ravichandran, J. Adhes. Sci. Technol. 29 (2015) 1465.
[29] U. Nazir, Z. Akhter, N.K. Janjua, M.A. Asghar, S. Kanwal, T.M. Butt, A. Sani, F. Liaqat, R. Hussain, and F.U. Shah, RSC Adv. 10 (2020) 7585.

[30] M. Acila, H. Bensabra, and M. Santamaria, Metall. Res. Technol. 118 (2021) 203.
[31] R. Rosliza, W.W. Nik, S. Izman, and Y. Prawoto, Curr. Appl. Phys. 10 (2010) 923-929.
[32] I.B. Onyeachu, I.B. Obot, and A.Y. Adesina, Corros. Sci. 168 (2020) 108589.
[33] G. Ji, S. Anjum, S. Sundaram, and R. Prakash, Corros. Sci. 90 (2015) 107-117.
[34] H. Ma, S. Chen, B. Yin, S. Zhao, and X. Liu, Corros. Sci. 45 (2003) 867-882.
[35] A. Ayoola, R. Babalola, B. Durodola, E. Alagbe, O. Agboola, and E. Adegbile, Results Eng. 15 (2022) 100490.
[36] A. Kokalj, Corros. Sci. 196 (2022) 109939.
[37] M. Faustin, A. Maciuk, P. Salvin, C. Roos, and M. Lebrini, Corros. Sci. 92 (2015) 7.
[38] M. Acila, H. Bensabra, and A. Saoudi, Rev. Roum. Chim. 66 (2021) 921.